CRCLEME

Cooperative Research Centre for
Landscape Environments
and Mineral Exploration

OPEN FILE
REPORT
SERIES

Australian Government
Geoscience Australia

Government
of South Australia
Department of Water,
Land and Biodiversity
Conservation

DETERMINING THE SUITABILITY OF IN-STREAM NANOTEM FOR DELINEATING ZONES OF SALT ACCESSION TO THE RIVER MURRAY: A REVIEW OF SURVEY RESULTS FROM LOXTON, SOUTH AUSTRALIA.

Kok Tan, Volmer Berens, Mike Hatch and Ken Lawrie

CRC LEME OPEN FILE REPORT 192

January 2007

CRCLEME

Report prepared for the Murray Darling Basin Commission (MDBC)
This project is co-funded by the MDBC and CRC LEME

CRC AUSTRALIA

Australian Government
Geoscience Australia

Government of South Australia
Department of Water, Land and Biodiversity Conservation

CRCLEME
Cooperative Research Centre for Landscape Environments and Mineral Exploration

DETERMINING THE SUITABILITY OF IN-STREAM NANOTEM FOR DELINEATING ZONES OF SALT ACCESSION TO THE RIVER MURRAY: A REVIEW OF SURVEY RESULTS FROM LOXTON, SOUTH AUSTRALIA.

Kok Tan, Volmer Berens, Mike Hatch and Ken Lawrie

CRC LEME OPEN FILE REPORT 192

January 2007

Report prepared for the Murray Darling Basin Commission (MDBC)
This project is co-funded by the MDBC and CRC LEME

CRC LEME is an unincorporated joint venture between CSIRO-Exploration & Mining, and Land & Water, The Australian National University, Curtin University of Technology, University of Adelaide, Geoscience Australia, Primary Industries and Resources SA, NSW Department of Primary Industries and Minerals Council of Australia.

Headquarters: CRC LEME c/o CSIRO Exploration and Mining, PO Box 1130, Bentley WA 6102, Australia

This Open File Report 192 has been produced by the CRC for Landscape Environments and Mineral Exploration.

Electronic copies of the publication in PDF format can be downloaded from the CRC LEME website: http://crcleme.org.au?Pubs?OFRindex.html. Information on this or other CRC LEME publications can be obtained from: http://crcleme.org.au

Hard copies will be retained in the Australian National Library, The State Library of Western Australia and the CSIRO Library at the Australian Resources Research Centre, Kensington, Western Australia.

Reference:
Tan, K, Berens, V, Hatch, M, and Lawrie, K, 2007. Determining the Suitability of In-Stream Nanotem for Delineating Zones of Salt Accession to the River Murray: A Review of Survey Results From Loxton, South Australia. *CRC LEME OFR 192.* pp 24.

1. In-stream NanoTEM - South Australia
2. Salt Accession - Murray River and Loxton, South Australia

CRC LEME Open File Report 192.
ISSN 1329-4768
ISBN 1 921039 531

Addresses and affiliations of authors:

Kok Tan
Geoscience Australia
GPO Box 378
CANBERRA ACT 2601
AUSTRALIA

Ken Lawrie
Geoscience Australia
GPO Box 378
CANBERRA ACT 2601
AUSTRALIA

Volmer Berens
Department of Water, Land and Biodiversity Conservation, SA
GPO Box 2834
ADELAIDE SA 5001
AUSTRALIA

Mike Hatch
Department of Geology and Geophysics
The University of Adelaide
ADELAIDE SA 5005
AUSTRALIA

Contents Page

List of Figures

Page

List of Tables Page

Acknowledgements

The authors would like to express their gratitude to Wei Yan (DWLBC) for the pertinent discussion on the hydrology of the Loxton-Bookpurnong area. Additional thanks to David Gibson, Colin Pain and Jeremy James of Geoscience Australia for reviewing this manuscript. The GIS inputs from Heike Apps and Larysa Halas are much appreciated.

Executive Summary

As part of an independent review, CRC LEME at Geoscience Australia (Canberra) was tasked by the Murray Darling Basin Commission (MDBC) to help determine the suitability of the NanoTEM system for delineating salt accession into the River Murray. CRCLEME were endorsed to join the instream coring program and are aware of the South Australian Department of Water Land and Biodiversity Conservation's (DWLBC) investigation to validate instream NanoTEM conductivity with river sediment pore fluid salinity. Data collected and analysed by each organisation during the investigation have proved valuable towards the assessment. Collaborative data and research of the instream program are used to examine relationship between conductivity, salinity and lithology.

Once successfully validated, the "in river" NanoTEM technique would be regarded as having considerable potential as a relatively cost-effective method for establishing the locations of major salt flux risk into the river system. The observed conductivity from the NanoTEM, when coupled with ground validation and hydrological modelling, is intended to be used to assist the various stake holders in implementing management and engineering options to attenuate salinity of both within the River Murray and its adjacent flood plains and creeks.

This report summarises the results of borehole and laboratory studies undertaken to validate the in-stream NanoTEM signatures with respect to the salinity and lithology in the river beds. Recommendations are made on the suitability of utilising in-stream NanoTEM to delineate salt accession into River Murray sediments.

The following major conclusions are drawn from this study:

1. The measured Cl^- and TDS of river sediment pore fluids correlate positively, which suggest that the former can be used as a surrogate for salinity.
2. Within the top 4 m of the river sediments, the measured nanoTEM data primarily reflects the pore fluid salinity as there are only small variations in the porosity of the sediment (Monoman Formation). In comparison, the electrical conductivity at greater depth (4 – 10 m) is a function of both salinity and porosity as the more porous muddy sand of the Bookpurnong Formation is present.
3. Conductivity values at less than 1 m sediment depth do not correlate with the pore fluid salinity, the former being less conductive than the high salinity of the pore fluids would suggest. This problem can be alleviated with better modelling.

In summary, the in-stream nanoTEM system results appear to provide a reliable measure of river sediment salinity, and can therefore be used to delineate the spatial distribution of salt accession risk along the River Murray. These data should be used within the context of an understanding of the hydrogeology of the area, and knowledge of the river bed sediment composition and texture is desirable to assist with data interpretation.

Some recommendations for further development/refinement and calibration of the in-river nanoTEM system are also made.

1. Introduction

The River Murray in South Australia has been under constant threat from discharging saline groundwater. On average, 173 tonnes/day of salt enters the river in the 40 km stretch between Loxton and Bookpurnong at low flows (5,000 ML/day), and up to 365 tonnes/day at high flows (20,000 – 30,000 ML/day) (Yan *et al*., 2005). The new Loxton salt interception scheme (SIS), which is currently in the process of being set up, will help remove a large portion of this water. However, the effectiveness of such a scheme depends on our ability to accurately locate areas of salt accession to the river.

Conventionally, salinity results from water monitoring stations located at 10 kilometre intervals along the river, and Run of River data at 1 km intervals (Porter, 2001) have been evaluated to determine those stretches of river most susceptible to salinisation. However, east of the river gorge, the presence of an extensive floodplain and a highly sinuous meandering river course produces a more complex hydrological scenario requiring a more thorough sampling strategy. As a result, the in-river NanoTEM was developed for the purpose of mapping the resistivity of the river sediments at a resolution high enough to delineate the salinity 'hot-spots' (Barret *et al.*, 2003; Middlemis *et al.*, 2004; Telfer *et al.*, 2004). DWLBC engaged Zonge Engineering to undertake a geophysical survey utilising the NanoTEM along a 35 km stretch of the river between the Katarapko Creek outlet and Lock 4 (Figure 1). To both validate the NanoTEM results and aid in establishing the hydrodynamics of the river system, a in-stream coring and sampling field program was developed and conducted by DWLBC (Berens et al., 2007)

As part of an independent review, CRC LEME at Geoscience Australia (Canberra) was tasked by the Murray Darling Basin Commission (MDBC) to help determine the suitability of the NanoTEM system for delineating salt accession into the River Murray. CRCLEME were endorsed to join the instream coring program and are aware of the South Australian Department of Water Land and Biodiversity Conservation's (DWLBC) investigation to validate instream NanoTEM conductivity with river sediment pore fluid salinity (Berens et al., 2007), with particular regard to the design and development of the Loxton Salt Interception Scheme (Howles et al., 2007). Data collected and analysed by each organisation during the investigation have proved valuable towards the assessment. Collaborative data and research of the instream program are used to examine relationship between conductivity, salinity and lithology.

Once successfully validated, the "in river" NanoTEM technique would be regarded as having considerable potential as a relatively cost-effective method for establishing the locations of major salt flux risk into the river system. The observed conductivity from the NanoTEM, when coupled with ground validation and hydrological modelling, is intended to be used to assist the various stake holders in implementing management and engineering options to attenuate salinity of both within the River Murray and its adjacent flood plains and creeks.

2. Objective

The study outlined in this report aims to determine whether near surface resistivity values acquired by the in-river NanoTEM method is caused by variations in salinity or is linked to changes in sedimentary textures and porosities.

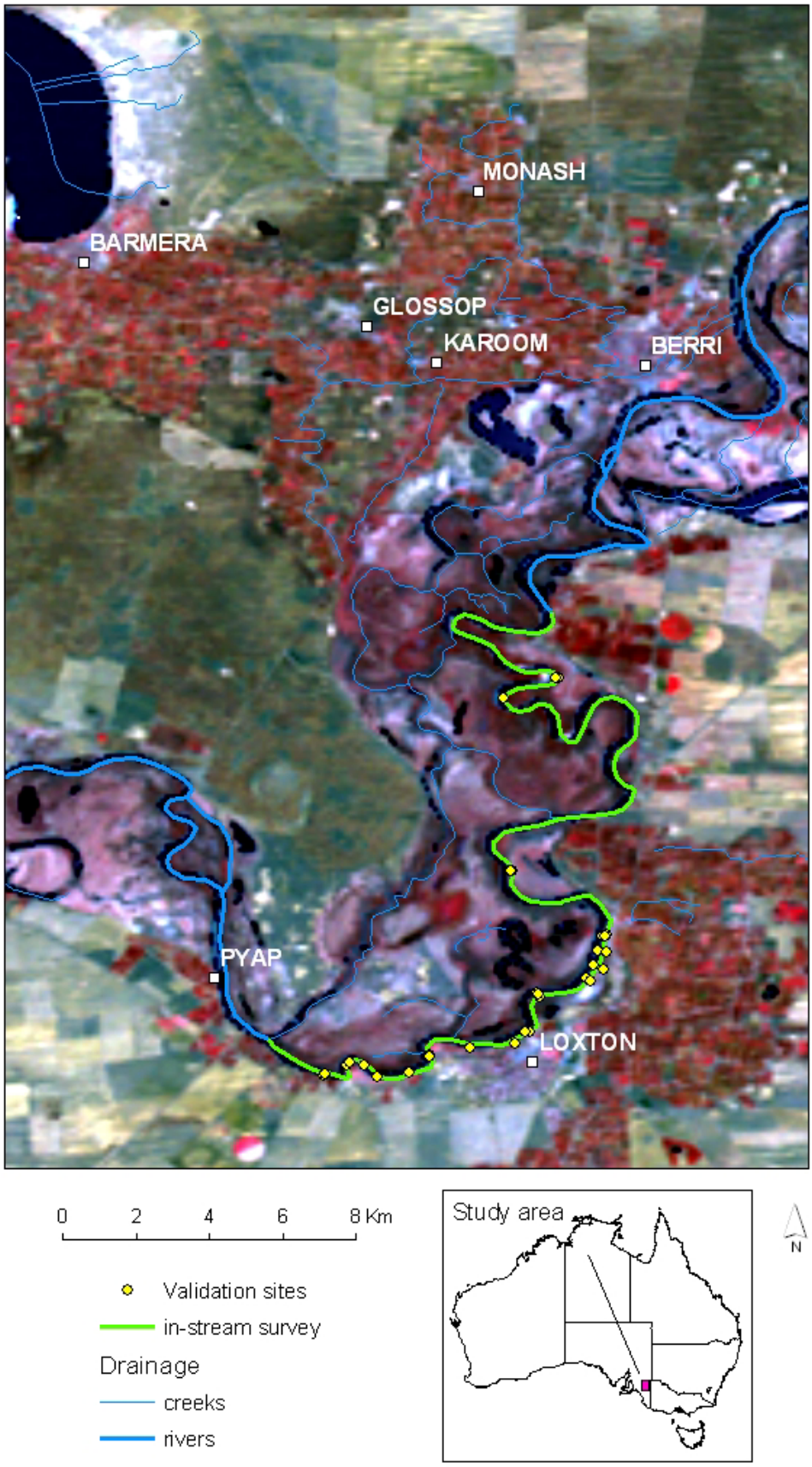

Figure 1. Landsat TM image showing study area and 35 km stretch of the river surveyed in September 2003 using the towed array NanoTEM system.

3. In-Stream NanoTEM

The geophysical equipment used in this study was a floating version of Zonge Engineering and Research Organisation's land-based NanoTEM system. This consisted of a 7.5 m x 7.5 m transmitter loop and a single 2.5 m x 2.5 m turn receiver loop (Figure 2). Both transmitter and receiver were mounted on a rigid floating PVC framework and towed behind a single motor boat. Data were acquired in a nearly continuous mode every 4 seconds using 64 cycles at a repetition rate of 32 Hz and a sampling rate of every 5 to 8 m along the river. Location was determined using a GPS/sounder which logged position and water depth at approximately every 10 m. All three datasets were time-stamped and synchronised to produce accurately-located TEM soundings and associated water depths (Berens *et al.*, 2004).

A total of 80 km of data were collected over a 35 km stretch of the river (Figure 1) between the Katarapko Creek outlet and Lock 4. The TEM data were inverted to provide vertical resistivity information down to 30 m. This process generally generates at least 10 resistivity depth values at each sounding (Figure 3) (Berens *et al.*, 2004).

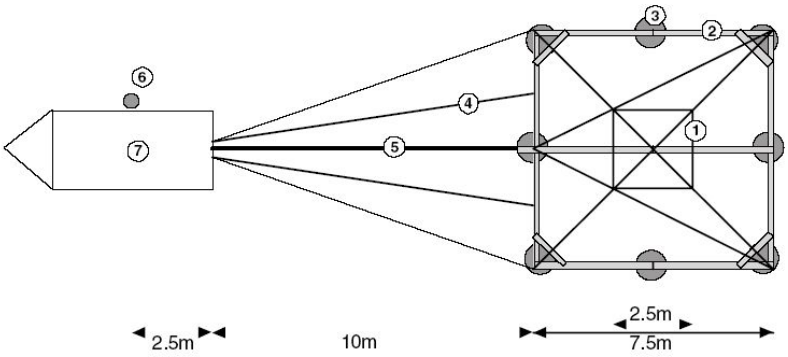

Figure 2. Towed NanoTEM array. Main components: receiver loop (1), transmitter loop (2), tyre inner tube (3), tow ropes (4), 10 m PVC towing spacer (5), GPS receiver (6), boat (7). Source: Barrett *et al.* (2003).

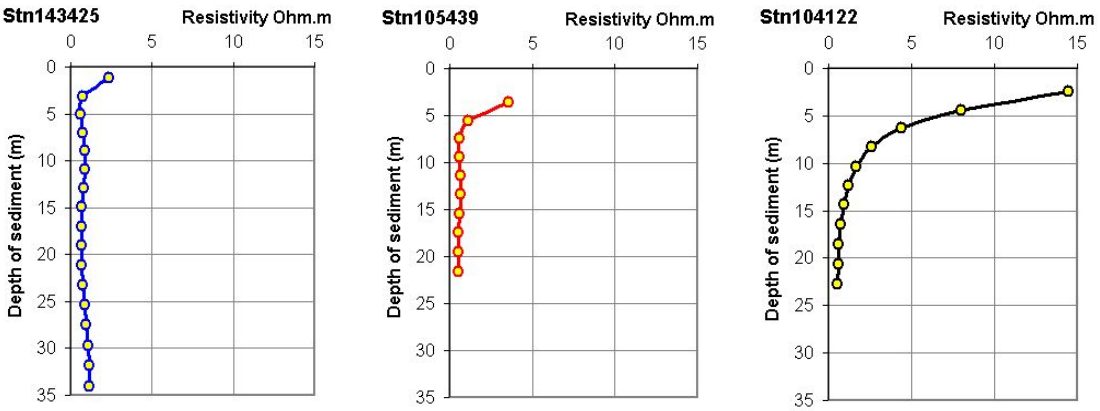

Figure 3. Three examples of resistivity profiles NanoTEM stations: 143425, 105439 and 104122. All are located in the vicinity of Loxton-Riverland cores (LRC) 12, 28 and 43 respectively.

3.1 River sediment resistivity results

The vertical resistivity profiles were stitched using Surfer™ to display as continuous lateral conductivity variations with depth (to ~ 30 m), data can also be presented three dimensionally using geographical information system (GIS) software (Figure 4) (Berens *et al.*, 2004). The image (Figure 4) revealed the presence of shallow resistive sediments at several locations. Nevertheless, these overlie highly conductive sediments.

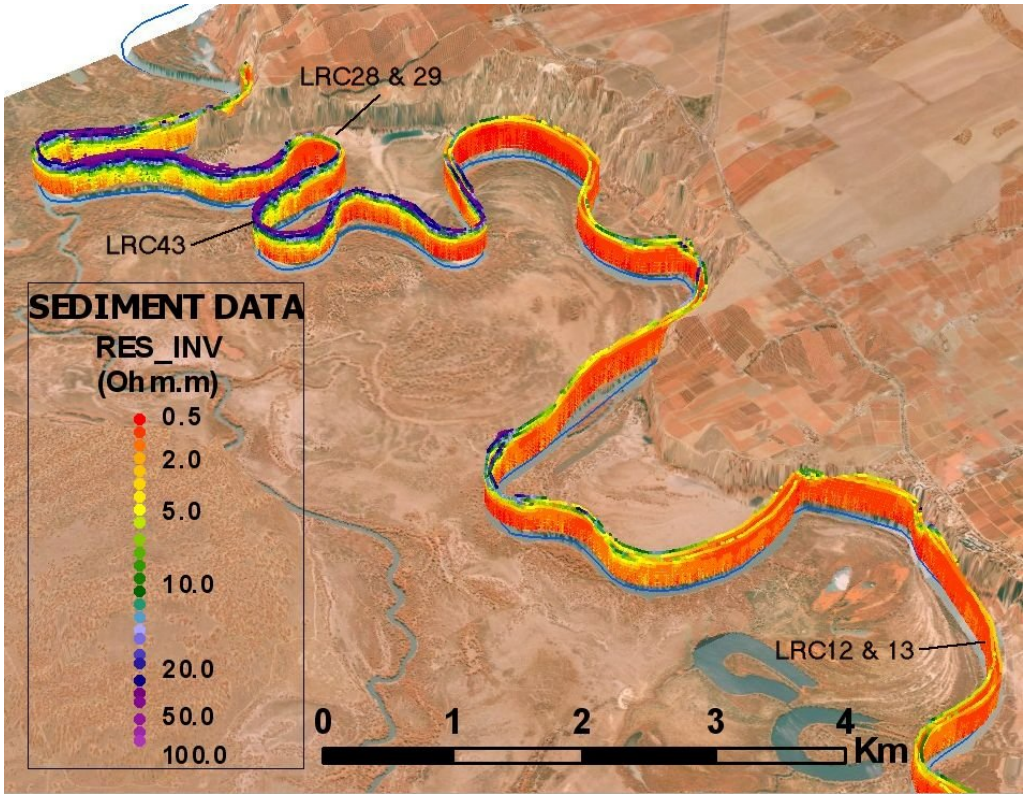

Figure 4. Oblique view of in-stream NanoTEM resistivity values along part of the Loxton-Bookpurnong survey section showing stretches of resistive (blue) and conductive (yellows and reds) zones within river sediments. Adapted from Berens and Hatch (in prep.).

4. Field Sampling Program

GeoCoastal Australia was contracted by DWLBC to drill 32 sites using a vibro-core system mounted on a modified fork-lift tractor with the vehicle secured and mobilised on a barge (Figure 5). At each site, coring was done to refusal (up to 10 m depth) with most holes terminating in mud. The vibro-core involves a hydraulic vibration head on top of a stainless steel barrel that vibrates downwards into the saturated sediments. Retrieved cores (60 mm diameter) were extruded using pressured air into plastic sleeves (Figure 6) for preservation and sampling.

Figure 5. Fork-lift tractor vibro-core system mounted on a barge.

Figure 6. Plastic sleeve containing extruded core for sampling and storage.

For each core, DWLBC staff collected samples every 0.2 m in top 2 m and 0.5 m samples there after. All were measured for chloride (Cl^-) concentrations and selection for major ions. A spoonful of sample was also collected and placed into chip trays for lithological logging.

For this review, representative samples were collected from sites LRC 11, 12, 13, 32, 98 and 99 (Table 1). These were split into triplicates for grain size distribution, mineralogy and porosity measurements. 30 cm cores were also collected and samples from a few of these had pore fluids extracted using hydraulic press. These were analysed for a suite of major cations and anions.

Table 1. Spatial coordinates and depths of the nine (of 26) validation boreholes. Coordinates are in GDA94, Zone 54.

Borehole	Easting	Northing	Total Depth m
LRC11	460772	6189460	5.6
LRC12	461858	6189930	6.8
LRC13	461945	6189855	5.9
LRC28	461149	6198097	10.0
LRC29	461205	6198118	6.7
LRC32	467048	6189509	6.0
LRC43	459948	6197555	8.5
LRC98	460483	6188450	6.0
LRC99	460483	6188450	6.8

5. Methods

The apparent electrical conductivity (EC_a) of a sample is influenced by the electrical conductivity of both the solid and liquid phases (Rhoades *et al.*, 1976). Amongst these, the saturated porosity of sediments (i.e. water content) and electrolyte concentrations of pore fluids (i.e. salinity) are the dominant factors (Tan *et al.*,2004). Thus, physical attributes of the sediments controlling the water content are important and therefore need to be characterised. In this study, validation of the in-stream NanoTEM results and field observations has undertaken in 3 steps:

- The porosity, texture and mineral composition, controlling the water content of sediments was examined
- Chloride concentrations were compared with the total dissolved solids (TDS). Once a positive relationship is established, Cl^- concentrations are then used as a surrogate for total salinity.
- Chloride data and predicted EC_a from five coring sites (LRC 12, 13, 28, 29, 43) (Table 1) was compared with the NanoTEM EC_a results to determine the accuracy of the latter for measuring salinity variations in the river sediment.

Mineral composition was analysed using X-ray diffraction (XRD) in the form of a Siemens D500 X-ray diffractometer. Semi-quantitative analysis of mineral composition was also calculated utilising the CSIRO's Siroquant software. Laser grain size analyses were undertaken using a Master Laser Particle-Sizer. Porosity measurements were carried out on known volumes of saturated samples from which the total water content was calculated by completely oven drying the samples. Details of the laboratory methods used are shown in Appendices 1 and 2.

6. Results

6.1. Textures and Mineral Composition

Borehole lithologies are summarised in Table 2 using the sedimentary classification system (Lewis and McConchie, 1994).

Table 2. Lithology description of the nine validation cores.

Borehole	Total Depth (m)	Lithology (Starting from the surface)
LRC11	5.6	2.5 m of well sorted fine sand; 0.5 m of poorly sorted fine to coarse sand; 2.6 m of grey sand, muddy sand and olive grey muddy sand with abundant shell fragments.
LRC12	6.8	5.3 m of moderately sorted fine to medium sand, and poorly sorted fine to coarse sand and granules; 1.5 m of olive grey muddy fine sand.
LRC13	5.9	5.5 m of fine to moderately sorted sand; 0.4 m of grey muddy sand.
LRC28	10.0	8.5 m of poorly sorted medium to coarse sand and granule; 1.5 m of olive grey muddy sand with shell fragments.
LRC29	6.7	6.7 m of poorly sorted fine/medium to coarse sand.
LRC32	6.0	4.5 m of Moderate to poorly sorted sand and granule; 1.5 m of grey sandy mud with shell fragments.
LRC43	8.5	6.5 m of poorly sorted medium to coarse sand; 2 m of grey muddy sand, partly cemented.
LRC98	6.0	4 m of poorly sorted fine to coarse sand; 2 m of grey muddy sand.
LRC99	6.8	5.6 m of moderately sorted fine and medium sand; 1.2 m of grey muddy sand with shell fragments.

The river sediments can be classified into four texture groups – dominated by sands (including granule-bearing variants) and muddy sand, with only one sample each of silty sand and silty mud (Figure 7). The sands (including the silty sand sample) are interpreted to belong to the Monoman Formation, while the muddy sand and silty mud are assigned to the lower Loxton clay. Essentially, the top 3 – 4 m of sediments are dominated by sand.

The sands of the Monoman Formation are composed dominantly of quartz (80 – > 95 wt. %), with < 2 wt. % of feldspar and < 10 wt. % muscovite.

The lower Loxton clay (muddy sand) contains approximately 60 – > 70 wt. % of carbonates (calcite, aragonite and ankerite). The remainder comprise quartz (6 -15 wt %), mica (up to 30 wt. % as illite), kaolinite (up to 18 wt. %), and feldspars (< 5 wt. %, K-feldspar dominant).

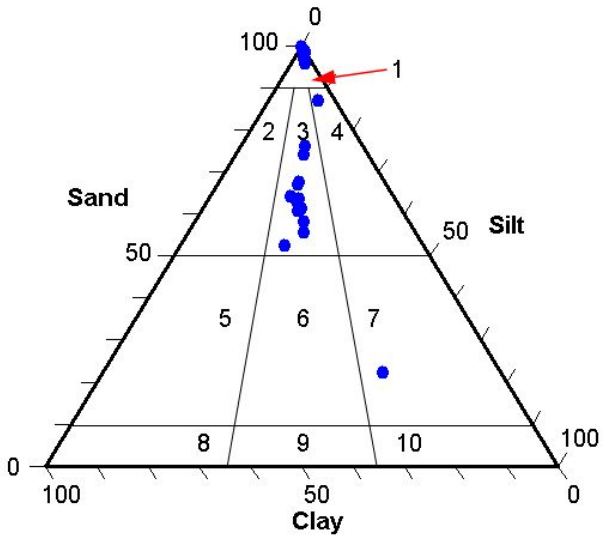

Legend:

1. Sand
2. clayey sand
3. muddy sand
4. silty sand
5. clayey mud
6. sandy mud
7. silty mud
8. clay
9. mud
10. silt

Figure 7. Ternary plot of grain size distribution data for the river sediments based on laser grain size analysis (clay < 4 μm). The sedimentary grain size grouping system after Lewis and McConchie (1994).

6.2. Porosity

In the saturated zone, total porosity of sediments controls the maximum water content. An external laboratory, Sydney Environmental and Soil Laboratory, independently measured the porosities of an additional 11 samples, and the results, together with the porosity measured using the syringe method (Appendix 2), are shown in Table 3.

There is a distinct porosity contrast between sands of the Monoman Formation and muddy sands of the lower Loxton clay. The porosities of the sands range from 26 to 39 vol %, with a median of 32 to 35 vol %, whereas the muddy sand ranges from 34 to 59 vol % porosity, with a median of 48 to 49 vol % (Table 3).

Table 3. Porosities of Monoman Formation sand and lower Loxton Clay muddy sand.

Porosity vol %	**Monoman Formation**		**lower Loxton Clay**	
	n = 23	**n = 5**	**n = 13**	**n = 6**
Minimum	26	*27*	34	*46*
Median	32	*35*	49	*48*
Maximum	36	*39*	59	*53*

NB: values in italics denote results obtained from an external laboratory.

6.3. Pore Fluid Chemistry and Salinity

The geochemistries of 5 samples of pore fluids extracted from the sediments were analysed using ICP-OES (Table 4). The pore fluids are classified as Na-Cl-SO_4 type, with Na and Cl accounting for 70 to 80 % of the TDS (Table 5). Chloride alone accounts for 40 to 49 % of the TDS, whereas Na accounts for 26 to 33 %. Other cations such as Ca, Mg and K have low abundance (1 to 4 % of TDS).

Amongst the major elements, scatter plots for both Na^+ and Cl^- against TDS show strong correlations (r^2 = 0.98 & 0.99 respectively) whereas those of SO_4^{2-} are positive but are less

well correlated ($r^2 = 0.82$) (Figures 8a, b & c). This suggests that Na^+ or Cl^- can be used as a surrogate to express salinity trends in the saturated sediments.

Table 4. Concentrations of major ions obtained from sediment pore fluids.

Borehole	Na^+ mg/l	Ca^{2+} mg/l	K^+ mg/l	Mg^{2+} mg/l	Cl^- mg/l	SO_4^{2-} mg/l	CO_3^{2-} mg/l	TDS mg/l
LRC 99	13,761	844	471	1709	21,509	9,975	70	48,452
LRC11	3,330	330	95	374	5,260	3,290	< 50	12,978
LRC14	16,825	801	341	1,118	26,110	8220	120	53,671
LRC98	11,800	325	377	760	16,600	6,250	94	36,358
LRC98	10,600	254	309	654	15,600	5,170	160	32,880

Table 5. Major ions expressed as a percentage of total dissolved solids (TDS).

Borehole	Na^+ %	Ca^{2+} %	K^+ %	Mg^{2+} %	Cl^- %	SO_4^{2-} %	CO_3^{2-} %	TDS mg/l
LRC 99	30	2	1	4	43	21	0.1	48,452
LRC11	26	2.5	1	3	40	25	<0.4	12,978
LRC14	31	1	1	2	49	15	0.2	53,671
LRC98	33	1	1	2	45	17	0.3	36,358
LRC98	32	1	1	2	47	15	0.5	32,880

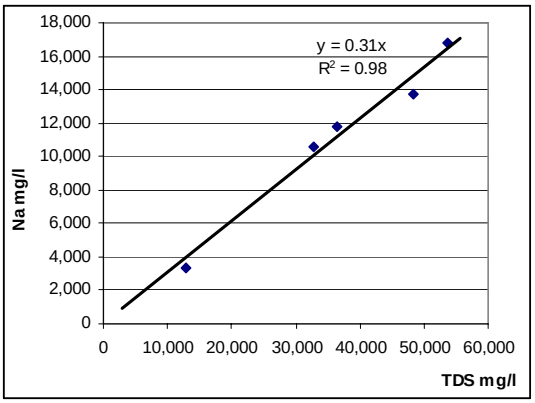

Figure 8a

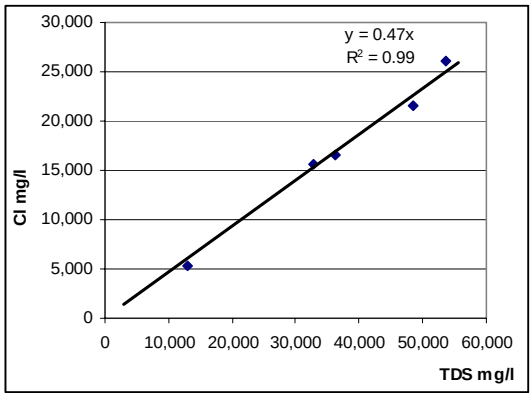

Figure 8b

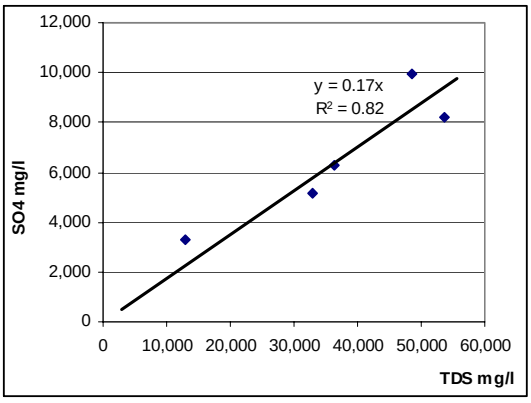

Figure 8c

Figures 8a – c. Scatter plots of Na^+, Cl^- and SO_4^{2-} against the total dissolved solids (TDS) respectively.

6.4. Salinity Trends in the Sediments

Measured salinity trends near the base of the river provide a basis for depicting the hydrodynamics of the river and groundwater interactions. Salt accession into the river would be related with high salinity pore water in the shallow river sediments whereas river water recharging into the sediments will tend to have low salinity pore water present in the shallow hyperitic zone.

Overall, salinity increases with depth. Of the sampled sites (Figure 9), sediment at LRC43 has the lowest salinity, with < 200 mg/l Cl^- for the top 6 m. LRC12 and LRC29 are highly saline, with Cl^- concentrations of 10,000 and 15,000 mg/l at the water-sediment interface, reaching > 20,000 mg/l at 1.5 m and 4 m respectively. At LRC28, salinities in the top 2 m of sediment remains consistent at 5,000 mg/l Cl^-, increasing gradually to 20,000 mg/l Cl^- at 6 m depth. In contrast, LRC13 is highly saline in the top half metre (10,000 mg/l Cl^-), gradually increasing to 15,000 mg/l at 5 m depth.

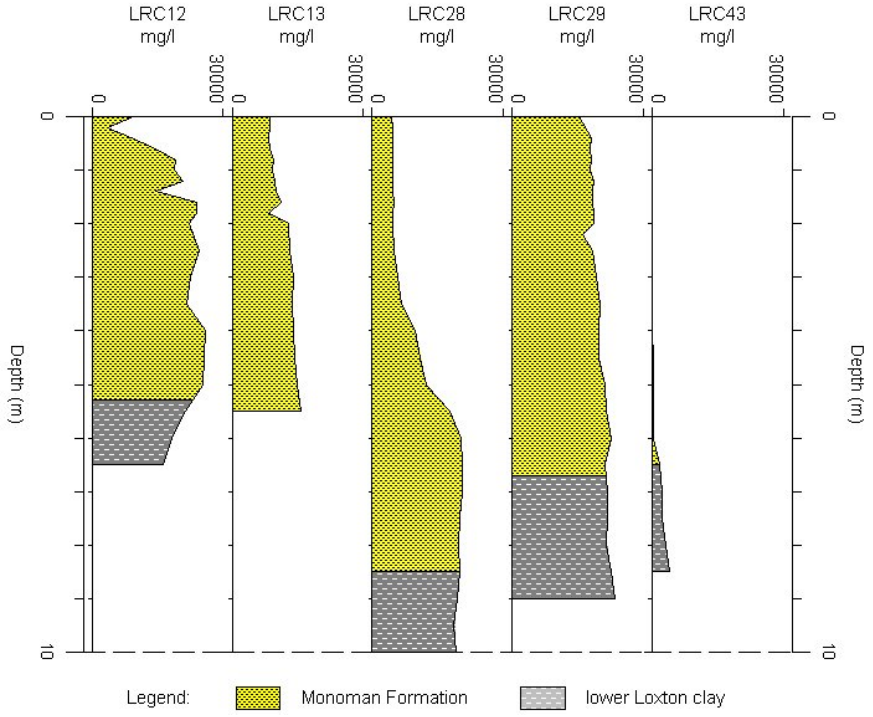

Figure 9. River bed sediment chloride concentration profiles and lithologic units at sites LRC12, LRC13, LRC28, LRC29 and LRC 43.

6.5. Correlation between In-stream NanoTEM Measurements and Salinity

The apparent electrical conductivity responses and spatial distribution of these signatures highlights the chemical and physical attributes of regolith materials and unweathered rock, with the latter largely resistive. Rhoades *et al.* (1976) demonstrated that the apparent conductivity of a material is the weighted summation of the electrical conductivity of both liquid and solid phases (Equation 1). In the absence of massive sulphides, conductivity is dominantly attributed to the liquid phase, which is in turn driven by the volumetric water content and the electrolyte (mainly sodium and chloride) ion concentration in the pore water.

$$EC_a = EC_w\theta\tau + EC_s \qquad \text{Equation 1}$$

(EC_a - apparent conductivity, EC_w - pore water conductivity, θ - volumetric water content, τ - tortuosity, EC_s - solid phase conductivity)

To validate the in-stream NanoTEM results, it is imperative to correlate the measured resistivity with the pore fluid salinity in the sediments. To ease in the interpretation of the correlation results, the measured resistivity (Ω.m) has been converted to electrical conductivity (mS/m) using the relationship 1 S/m = 1/Ω.m. Plotting electrical conductivity against chloride concentration shows a positive correlation (r^2 = 0.6) (Figure 10a). The presence of outlying data are mainly associated with very shallow sand < 1 m below the river bed, indicating that the in-river NanoTEM has underestimated conductivities at the water-sediment interface. This is attributed to the fact that the data inversion process of the NanoTEM technique can not accurately resolve the conductivity change at the sharp river and sediment interface. Re-plotting the conductivity against salinity for the Monoman Formation sand (> 1 m depth) yields an improved correlation (Figure 10b) and confirms that the observed resistivity response is caused mainly by salinity variations. The correlation between the chloride data from the lower Loxton clay and resistivity (Figure 10a) also supports this finding.

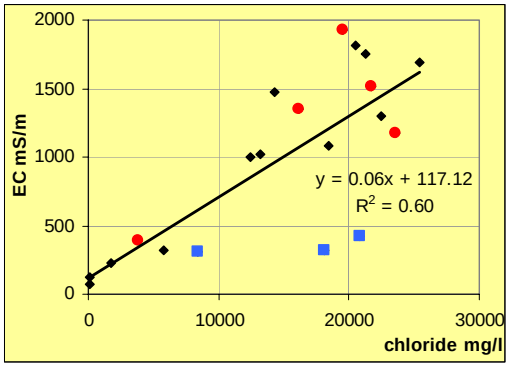

Figure 10a. Scatter plot of observed NanoTEM conductivities for river sediments versus chloride contents. Blue squares denote sand at < 1m depth (below the river bed) and red circles depict lower Loxton clay.

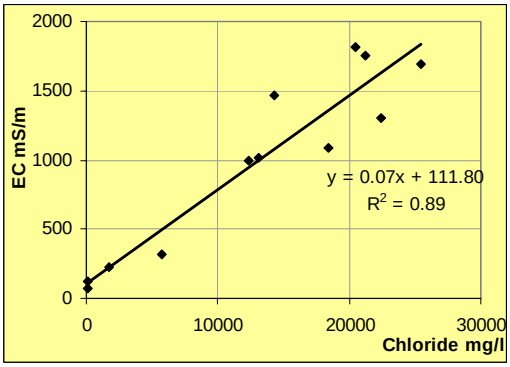

Figure 10b. Scatter plot of observed NanoTEM conductivities versus Monoman Formation sand chloride content at depths > 1 m below the river bed.

7. Discussion

The Monoman Formation sand and lower Loxton clay muddy sand texture groups individually appear to exhibit fairly constant internal porosities, with the later formation generally having higher porosities than the former. This has significant implications for interpretation of the NanoTEM conductivity results as EC_a is a function of salinity and water content, the latter being equivalent to the porosity under saturated conditions. Thus, when little difference in porosity is detected n the top 4 m of sediment (*i.e.* sand), variations in EC_a across different parts of the river system reflect changes in pore fluid salinity. This is supported by the study results, which suggest that the most likely cause of observed resistivity variations in the sediments at shallow depth is due to differences in salt concentration. At greater depths however, an increase in salinity and a change to more porous lower Loxton clays in most areas is accompanied by an increase in conductivity.

Thus, shallow conductive zones (<5 Ωm.m) are interpreted as alluvium saturated with saline groundwater. On the other hand, resistive areas (>10 Ωm.m) indicate the presence of fresher

river water recharging into the underlying sediments (Figure 11). According to the in-river resistivity data, areas close to the Loxton irrigation zone and where the river meanders eastwards towards the irrigation induced groundwater mound, are susceptible to heightened rates of salt accession. These regions have been targeted for SIS development. In comparison, distant areas, especially where the river meanders away from the highlands, are characterised by fresh river water recharging the river sediments.

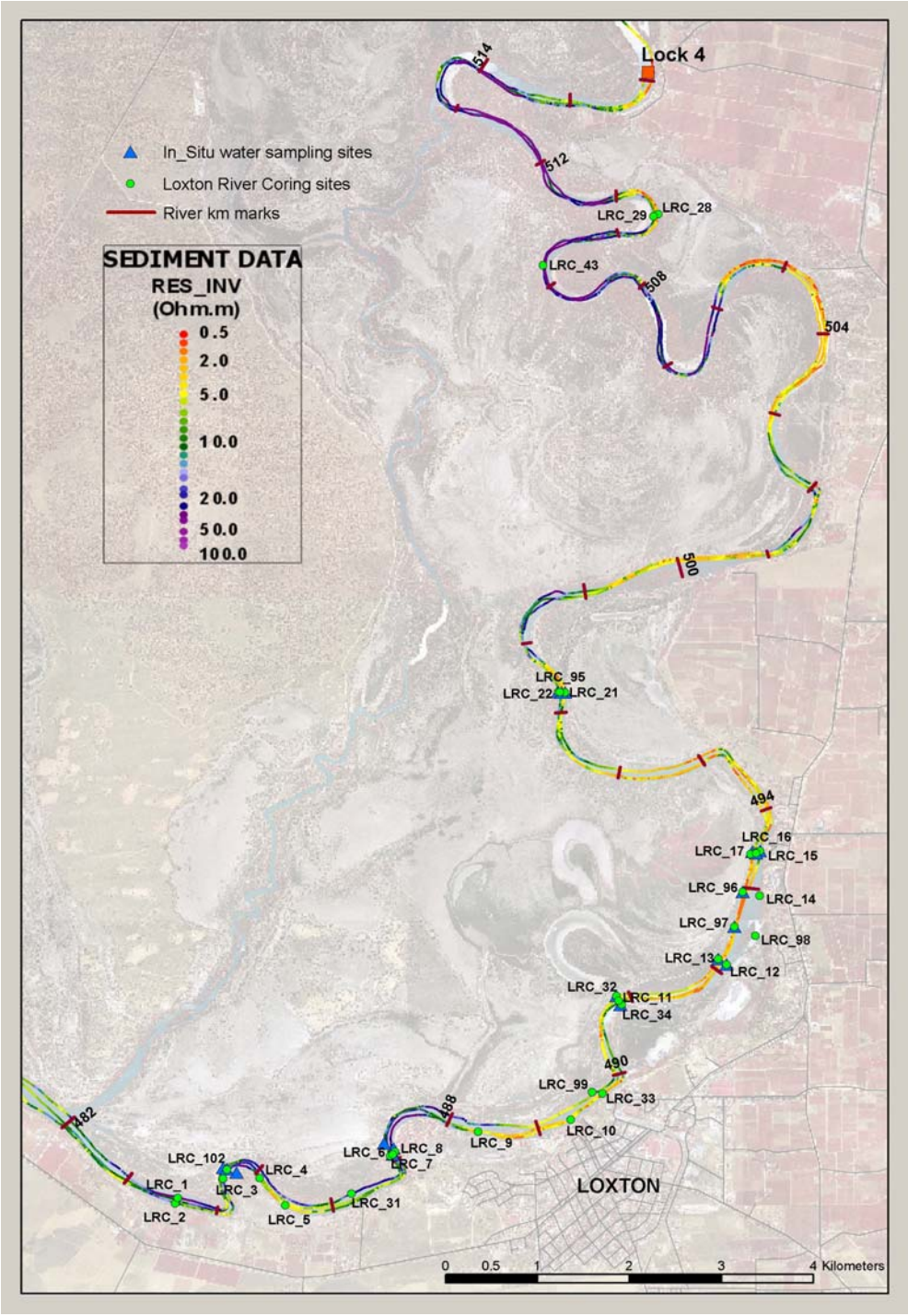

Figure 11. NanoTEM results along a 35 km stretch of the Murray River. Also shown are the 32 validation coring sites. Yellow and red colours are conductive zones, whereas blues are resistive zones. (Source: DWLBC)

8. Conclusions and Recommendations

The following main conclusions are drawn from the current study:

1. The measured Cl^- and TDS of river sediment pore fluids correlate positively, which suggest that the former can be used as a surrogate for salinity.
2. Within the top 4 m, the measured nanoTEM data primarily reflects pore fluid salinity as there are only small variations in Monoman Formation sediment porosities. In comparison, electrical conductivity at greater depths (4 – 10 m) is a function of both salinity and porosity as the more porous muddy sand of the lower Loxton clay is present.
3. Conductivity values in sediments at < 1 m depth do not correlate accurately with pore fluid salinity, underestimating the conductivity with respect to the high salinity of the pore fluids. This is attributed to the NanoTEM data processing being unable to accurately resolve the conductivity at the thin interface.

In summary, the in-stream nanoTEM results appear to reflect the salinity of the river sediments and can therefore be used to delineate the spatial distribution of salt accession along the Murray River. These data should be used within the context of an understanding of the hydrogeology of the area. In particular, some knowledge of the river bed sediment composition and texture is desirable to assist with data interpretation.

Recommendations for further research into the nanoTEM system have been made by Mike Hatch (CRC LEME PhD student). These are listed below, and may form part of his PhD project.

1. To derive a more cost-effective method (e.g. utilising a “conductivity spear”) for ground truthing the in-stream NanoTEM.
2. To better calibrate the NanoTEM system with particular attention paid to the decay functions of the resistivity data in the early time-windows and the rectification of any anomalous values.
3. To trial the NanoTEM in different environments to determine how the system responds to anomalous salinity levels (e.g. towing the array in the sea).
4. To improve inversion of the resistivity data by constraining the parameters of the surface layer.

9. References

Barrett, B., Hatch, M., Heinson, G. and Telfer, A. 2003. Salinity monitoring of the Murray River using a towed TEM array. In Proceedings: Australian Society of Exploration Geophysicists, February 2003, Adelaide. 4 p.

Berens, V., Hatch, M., James-Smith, J. and Love, A. 2004. In-stream geophysics aiding the hydrogeological investigation for the Loxton salt interception scheme, SA. In Proceedings: Inaugural Australasian Hydrogeology Research Conference, November 2003, Melbourne. 3 p.

Berens, V. and Hatch, M. (in prep.). Ground-truthing in-stream transient electromagnetic data: correlating resistivity with riverbed pore water salinity: Australian Journal of Earth Sciences.

Berens, V., Hatch, M., James-Smith, J. and Love, A. 2007 (in prep). Loxton - Bookpurnong instream NanoTEM survey and validation using river sediment cores. Department of Water, Land and Biodiversity Conservation. Report DWLBC 2007/10.

Howles, S., Smith, A., Stadter, M., Yan, W., and Hill, A. 2007. Loxton Salt Interception Scheme well field design and construction report - Floodplain component. Department of Water, Land and Biodiversity Conservation. Report DWLBC 2007/06.

Moore, D.M. and Reynolds, Jr. R.C. 1989. X-ray Diffraction and the Identification of Clay Minerals, Oxford University Press, Oxford.

Lewis, D.W. and McConchie, D. 1994. Practical Sedimentology. Chapman and Hall, New York. 213 pp.

Middlemis, H., Jolly, I., Georgiou, J. and Walker, G. 2004. Groundwater modeling of salt interception schemes in the Woolpunda – Cadell reach of the River Murray. Rural soulutions, South Australia. 158 p.

Porter, B., 2001. Run of River salinity surveys - A method of measuring salt load accessions to the River Murray on a kilometre by kilometre basis. In Proceedings: 8th Murray Darling Basin Groundwater Workshop, September 2001 , Victor Harbour, South Australia. 6 p.

Rawle, A. 2001. Basic Principles of Particle Size Analysis: Technical Paper MRK043, Malvern Instruments Limited.

Rhoades, J.D., Raats, P.A.C. and Prather, R.S. 1976. Effects of Liquid-Phase Electrical Conductivity, Water Content, and Surface Conductivity on Bulk Soil Electrical Conductivity: Soil Science Society of America Journal, 40, 651-665.

Tan, K.P., Munday, T., Gibson, D. and Apps, H. 2004. The relationships amongst the moisture content, pore water salinity, texture, and the apparent electrical conductivity of regolith – evidence from the Riverland and Tintinara airborne EM projects. In Proceedings: CRC LEME Regional Regolith Symposia, November 2004. Canberra. 5 p.

Telfer, A.L., Hatch, M.A., Palfreyman, C.J. and Berens, V. 2004. Instream NanoTEM survey of the River Murray 2004: Blanchetown to Mallee Cliffs. Australian Water Environments Report No. 42417b. Prepared for the MDBC and the Mallee Catchment Management Authority. 97 p.

Yan, W., Howles, S., Howe, B. and Hill, A. 2005. Prediction of salt load entering the River Murray in the Loxton-Bookpurnong area. Department of Water, land and Biodiversity. Report DWLBC 2005/17. 240 p.

10. Appendices

Appendix 1 – Analytical Methods

10.1 Grain Size Distribution

Information on grain size distribution enables textural information to be validated, helps in the interpretation of sedimentary environments, and allows relationships between sedimentary texture and NanoTEM resistivity data and salinity to be established. 36 samples, each weighing approximately 20 g, were analysed for particle size using the Mastersizer™ laser diffraction instrument produced by Malvern Instruments (Figure A1). The results are shown in Table A2.

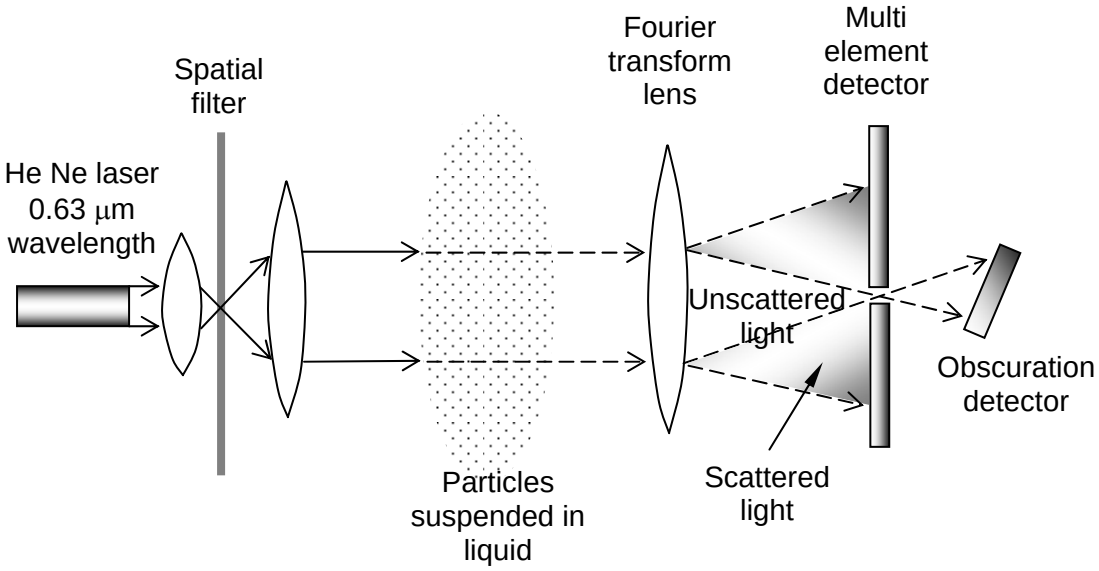

Figure A1. Schematic diagram showing the main components of a laser diffractometer. This technique allows the calculation of size fractions in volume % rather than weight %, such as those calculated using the sieving method. Source: Rawle (2001)

Table A1. Particle size in SI units (μm), Wentworth's scale.

Size Fraction	Lower boundary	Upper boundary
Very coarse sand	1000	2000
Coarse sand	500	1000
Medium sand	250	500
Fine sand	125	250
Very fine sand	62.5	125
Coarse silt	31	62.5
Medium silt	15.6	31
Fine silt	7.8	15.6
Very fine silt	4	7.8
Clay	0.05*	4

NB: * Detection limit.

The laser diffraction instrument consists of three parts: a laser source (He-Ne gas or diodes emitter), detectors, and a sample chamber that allows suspended particles to recirculate in front of the laser beam (Figure A1). The Mie theory (Rawle, 2001) was used to solve the equations for interaction of light with matter and calculates the volume of the particle. This technique calculates the % volume of a range of particle sizes (0.05 – 2000 μm), and the results are grouped according to the Wentworth's scale. To standardise with other analytical data, SI units (μm) were reported instead of Phi units (Table A1, Appendix 2).

10.2 Mineral Composition

Thirty-three samples were analysed for mineral composition, using the X-ray diffraction (XRD) technique. Individual samples were homogenised before approximately 5 g was removed and ground in a mortar with a pestle with ethanol to produce a fine, talc-like consistency (1-10 μm) so as to optimise the diffraction process (Moore and Reynolds, 1989). Each finely crushed sample was dried and randomly packed into a U-shaped aluminium holder covered with a frosted glass slide (to overcome preferred orientation of crystallites). The glass slide was then removed and most samples were analysed using a Siemens™ D5000 series X-ray diffractometer (Co-Kα), and scanned from 4 ^{o} to 80 ^{o} 2θ, at a speed of 2 ^{o} per minute, and a step size of 0.02 ^{o}. The remainder were analysed using a Siemens™ D501 (Cu-Kα), and scanned from 2 ^{o} to 70 ^{o} 2θ with the same settings as above.

Mineral identification software (EVA™) was used to identify the d-spacings of a series of peaks corresponding to individual minerals, and the mineral abundances were then quantified using SIROQUANT™ software.

10.3 Porosity Measurements

Graduated 60 ml syringes were sawn off at the tip, and pushed into saturated cores to obtain sample core plugs. The volume of the extracted plug was recorded and the wet samples were extruded from the syringe and placed onto aluminium foil dishes and weighed. These were then placed in an oven and left overnight at 105 ^{o}C. On the following day, the dried samples were taken out of the oven, placed in a desiccator and left to cool. These were then weighed and the moisture content calculated by difference. Since the weight of the fluid in grams is equal to its volume in millilitres at laboratory conditions, this volume was then divided by the wet sample volume to derive a % volume. At saturation, the volume of moisture is equivalent to the total porosity.

Appendix 2 – Analytical Results

Table A2. Tabulated results of grain size distribution, according to Wentworth's scale, and porosity. Size classes are in micrometre (μm) and porosity is in volume %.

Borehole	Depth m	Clay <4	Silt 4 - 62.5	Fine sand 62.5 - 250	Medium Sand 250 – 500	C / VC Sand 500 – 2000	Granule > 2000	Vol % Porosity	Interpreted Unit
LRC 11	2.8	2.2	10.5	51.8	26.9	5.4	3.2	35.1	Monoman Fm
LRC 11	4.0	0.9	3.0	6.0	16.2	67.2	7.1	25.8	Monoman Fm
LRC 11	4.2	9.4	16.5	41.3	19.6	13.3	0.0	35.1	lower Loxton clay
LRC 11	4.7	12.7	19.9	37.2	20.4	9.8	0.0	49.0	lower Loxton clay
LRC 11	4.8	6.7	16.1	27.5	30.4	14.3	5.3	34.0	lower Loxton clay
LRC 11	5.0	19.5	27.9	29.8	12.3	9.9	0.5	40.5	lower Loxton clay
LRC12	2.3	0.0	0.0	0.6	39.6	59.8	0.0	30.1	Monoman Fm
LRC12	2.4	0.0	0.0	1.6	36.3	61.4	0.7	32.6	Monoman Fm
LRC12	2.7	0.0	0.0	1.2	39.7	59.0	0.0	35.3	Monoman Fm
LRC12	2.8	0.0	0.0	6.6	38.5	54.6	0.3	27.1	Monoman Fm
LRC12	2.9	0.0	0.0	2.1	43.9	54.0	0.0	31.0	Monoman Fm
LRC12	3.2	0.0	0.0	0.4	31.3	67.9	0.4	31.6	Monoman Fm
LRC12	3.7	0.0	0.0	1.8	33.4	62.4	2.5	31.7	Monoman Fm
LRC12	4.2	0.0	1.0	7.3	35.5	54.4	1.8	28.3	Monoman Fm
LRC12	4.7	0.0	1.7	12.5	41.2	44.6	0.0	30.5	Monoman Fm
LRC32	2.3	0.0	0.1	3.2	34.9	61.2	0.5	33.1	Monoman Fm
LRC32	2.4	0.5	2.8	18.3	25.9	50.8	1.7	28.5	Monoman Fm
LRC13	2.3	0.3	1.8	5.1	26.8	66.0	0.0	30.2	Monoman Fm
LRC13	2.7	0.2	0.9	7.5	26.1	65.3	0.0	29.3	Monoman Fm
LRC13	3.2	0.0	0.0	17.3	42.7	39.7	0.3	31.0	Monoman Fm
LRC13	3.7	0.0	0.0	1.9	36.7	61.2	0.2	32.9	Monoman Fm
LRC13	3.8	0.4	2.8	23.1	56.4	17.3	0.0	35.7	Monoman Fm
LRC13	5.5	16.7	25.4	53.7	3.3	0.9	0.0	48.9	lower Loxton clay
LRC13	5.6	16.8	19.1	55.9	5.3	2.9	0.0	50.3	lower Loxton clay
LRC13	5.7	17.8	26.6	52.5	2.8	0.3	0.0	58.7	lower Loxton clay
LRC13	5.8	16.2	22.7	57.7	3.4	0.0	0.0	57.6	lower Loxton clay
LRC13	5.9	14.4	18.8	59.6	5.9	1.3	0.0	53.4	lower Loxton clay
LRC98	6.2	15.9	62.0	20.6	1.0	0.5	0.0	44.7	lower Loxton clay
LRC99	2.2	0.0	0.0	6.8	64.1	29.1	0.0	34.8	Monoman Fm
LRC99	2.7	0.0	0.0	4.3	42.7	52.3	0.7	33.4	Monoman Fm
LRC99	3.2	0.0	0.0	7.7	63.9	28.4	0.0	32.3	Monoman Fm
LRC99	3.7	0.0	0.0	6.5	65.3	28.2	0.0	32.4	Monoman Fm
LRC99	5.2	0.0	1.3	5.0	29.8	63.4	0.6	32.3	Monoman Fm
LRC99	5.7	16.2	20.8	59.4	3.4	0.2	0.0	48.7	lower Loxton clay
LRC99	6.2	17.0	22.5	56.4	3.1	1.0	0.0	53.7	lower Loxton clay
LRC99	6.3	16.1	20.3	59.5	3.3	0.8	0.0	54.7	lower Loxton clay

Table A3. Tabulated results of mineral composition and abundances (in weight %).

Borehole	Depth m	Quartz	Calcite	Aragonite	Siderite/ ankerite	Kaolinite	Mica	Feldspar	Others	Interpreted Unit
LRC11	2.3	78	0	0	0	1	11	8	2	Monoman Fm
LRC11	2.7	93	0	0	0	0	1	6	0	Monoman Fm
LRC11	3.2	80	0	0	0	0	6	9	4	Monoman Fm
LRC11	3.7	89	0	0	0	0	0	10	1	Monoman Fm
LRC11	3.9	84	0	2	0	0	5	9	0	Monoman Fm
LRC11	4.7	59	0	0	0	11	21	8	1	lower Loxton clay
LRC12	2.4	91	0	0	0	0	1	6	2	Monoman Fm
LRC12	3.2	96	0	0	0	0	0	4	1	Monoman Fm
LRC12	3.7	93	0	0	0	0	2	4	1	Monoman Fm
LRC12	5.5	8	49	28	0	6	7	0	1	lower Loxton clay
LRC12	5.8	16	40	16	0	6	15	4	3	lower Loxton clay
LRC12	6.0	32	22	10	0	6	27	0	2	lower Loxton clay
LRC12	6.2	13	45	15	0	6	20	0	1	lower Loxton clay
LRC32	2.3	96	0	0	0	0	0	4	0	Monoman Fm
LRC32	2.4	99	0	0	0	0	0	1	0	Monoman Fm
LRC13	2.7	96	0	0	0	0	0	4	0	Monoman Fm
LRC13	3.2	95	0	0	0	0	0	4	1	Monoman Fm
LRC13	3.7	97	0	0	0	0	0	3	0	Monoman Fm
LRC13	3.8	95	0	0	0	0	0	5	0	Monoman Fm
LRC13	4.0	93	0	0	0	0	1	6	0	Monoman Fm
LRC13	5.5	6	69	13	6	5	0	0	1	lower Loxton clay
LRC13	5.6	44	33	13	5	2	0	0	2	lower Loxton clay
LRC13	5.7	9	65	9	11	5	0	0	1	lower Loxton clay
LRC13	5.8	11	62	10	10	6	0	0	1	lower Loxton clay
LRC13	5.9	30	43	11	7	0	3	5	2	lower Loxton clay
LRC98	6.2	51	0	0	0	9	31	8	1	lower Loxton clay
LRC99	2.7	98	0	0	0	0	0	2	0	Monoman Fm
LRC99	3.2	94	0	0	0	0	0	5	1	Monoman Fm
LRC99	5.7	4	69	18	2	7	0	0	0	lower Loxton clay
LRC99	5.9	24	30	15	0	7	24	0	1	lower Loxton clay
LRC99	6.2	9	59	22	2	7	0	0	1	lower Loxton clay
LRC99	6.3	6	53	23	2	6	9	2	0	lower Loxton clay
LRC99	6.5	8	66	21	1	5	0	0	0	lower Loxton clay

Table A4. Tabulated in-stream NanoTEM resistivity data and calculated total dissolved solids (TDS).

Borehole	Sediment Depth m	NanoTEM Ωm.m	NanoTEM mS/m	Chloride mg/l	Calculated TDS mg/l
LRC12	1.2	2.36	424	20890	44496
LRC12	3.1	0.77	1299	22444	47806
LRC12	5.0	0.59	1695	25408	54119
LRC12	7.0	0.74	1351	16135	34368
LRC43	2.5	14.47	69	76	162
LRC43	4.5	7.98	125	92	196
LRC43	6.5	4.37	229	1769	3768
LRC43	8.5	2.57	389	3798	8090
LRC28	3.6	3.12	321	5760	12269
LRC28	5.6	1.00	1000	12386	26382
LRC28	7.5	0.55	1818	20476	43614
LRC28	9.5	0.52	1923	19477	41486
LRC13	0.5	3.27	306	8418	17930
LRC13	2.5	0.98	1020	13158	28027
LRC13	4.6	0.68	1471	14266	30387
LRC29	0.7	3.09	324	18087	38525
LRC29	2.8	0.92	1087	18382	39154
LRC29	4.9	0.57	1754	21260	45284
LRC29	7.0	0.66	1515	21688	46195
LRC29	9.0	0.85	1176	23570	50204

Source: In-stream NanoTEM data and chloride concentrations are provided by DWLBC.